Vukoslavčević, P. V., Wallace, J. M.: On the Accuracy of Measurement of Turbulent ...
THERMAL SCIENCE: Year 2017, Vol. 21, Suppl. 3, pp. S533-S551

S533

ON THE ACCURACY OF MEASUREMENT OF TURBULENT VELOCITY GRADIENT STATISTICS WITH HOT-WIRE PROBES

by

Petar V. VUKOSLAVČEVIĆ[a] and James M. WALLACE[b]*

[a] Department of Mechanical Engineering, University of Montenegro, Podgorica, Montenegro
[b] Burgers Program for Fluid Dynamics, Department of Mechanical Engineering,
University of Maryland, College Park, Md., USA

A very high resolution minimal channel flow direct numerical simulation was used to examine, virtually, the ability of various multi-sensor hot-wire probe configurations to measure the statistics of velocity gradient components. Various array and sensor configurations and the spatial resolution of probes with these configurations were studied, building on designs and investigations of various authors. In contrast to our previous studies, which focused on turbulent vorticity, vorticity-velocity correlations, dissipation and production rate, here the measurement accuracy of each component of the velocity vector gradient tensor is analyzed separately. The results of the study show that the virtual experiments compare well with a physical experiment, and that such virtual experiments are a powerful tool to examine the accuracy of velocity gradient measurements. The cross-stream gradients needed to determine the vorticity components can be measured with sufficient accuracy with most of the array and sensor configurations of vorticity probes used so far. A systematic error of some of the gradient measurements can appear due to the array or sensor configurations. None of the examined probe designs can measure, with sufficient accuracy, the streamwise velocity gradients, directly or indirectly, using the continuity equation.

Key words: *multi-array hot-wire probes, virtual experiments,*
           velocity gradient measurements, probe configurations,
           spatial resolution

Introduction

The first successful simultaneous measurement of the cross-stream velocity gradients were made by multi-sensor hot wire probes. These probes were designed to simultaneously measure all three vorticity components. Three or four sensors were arranged in three or more arrays displaced over small distances in the cross-stream y- and z-directions. By simultaneous measuring of all three velocity components at the center of each array, the velocity gradients in the cross-stream plane could be estimated by finite difference. The streamwise velocity gradients were estimated using Taylor's hypothesis [1] of frozen turbulence. Another possibility to estimate the streamwise gradients was to use an additional array placed at a

---

* Corresponding author, e-mail: petarv@ac.me

S534

Vukoslavčević, P. V., Wallace, J. M.: On the Accuracy of Measurement of Turbulent ...
THERMAL SCIENCE: Year 2017, Vol. 21, Suppl. 3, pp. S533-S551

close upstream distance from the arrays in the downstream cross-stream plane. Typical array and sensor configurations used to measure vorticity components, shown in fig. 1, are discussed by Wallace and Vukoslavčević [2]. The same set of convenient abbreviations, as the one used by Vukoslavčević and Wallace [3], is used here to label the various configurations. They consist of the first letters of the names of authors who designed and used them and the number of arrays for each probe.
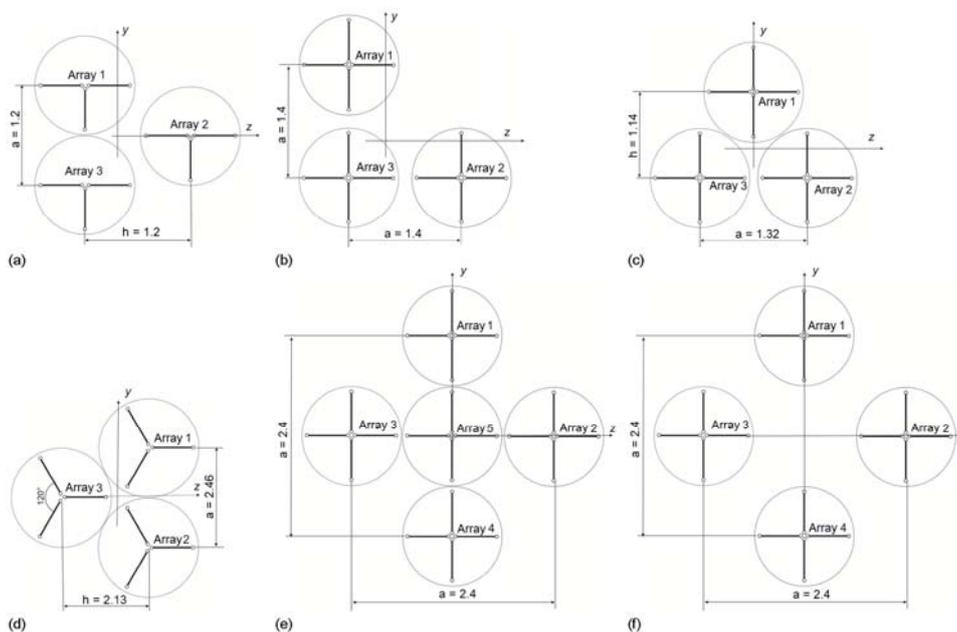

Figure 1. Various array configurations of multi-sensor hot-wire probes;
(a) VWB3, (b) TKD3, (c) VW3, (d) HA3, (e) TKD5, (f) TKD4

The configuration VWB3 was used by Vukoslavčević *et al*. [4], configurations TKD3 and TKD5 by Tsinober *et al*. [5], VW3 by Vukoslavčević and Wallace [6] and HA3 by Honkan and Andreopoulos [7]. Configuration TKD5, with the central array moved upstream of the other four arrays, was used by Galanti *et al*. [8] and by Gulitski *et al*. [9]. Configuration TKD4 was used as a part of the TKD5 configuration.

The influence of the geometrical configuration and number of the sensors within an array on the measurement accuracy of velocity components have been studied by many authors, who mainly focused on just a single array. A recent study of this type was carried out by Vukoslavčević and Wallace [10] and Vukoslavčević [11]. The only attempt to analyze the best array configuration was done by Vukoslavčević and Wallace [3]. They focused primarily on the accuracy of measurements of vorticity, vorticity-velocity correlations and turbulent kinetic energy dissipation and production and they also tested the accuracy of using Taylor's hypothesis. An analysis of the simultaneous influence of array arrangements within a probe and sensor arrangements within arrays on the accuracy of the vorticity and velocity-vorticity correlation measurements was also presented by Vukoslavčević and Wallace [12].

The aim of this study is to analyze the influence of the sensor arrangements within an array, the array arrangement within a probe sensing area, the probe spatial resolution and

Vukoslavčević, P. V., Wallace, J. M.: On the Accuracy of Measurement of Turbulent ...
THERMAL SCIENCE: Year 2017, Vol. 21, Suppl. 3, pp. S533-S551

S535

the ratio of the array to the array separation size on the accuracy of the measurement of each component of the velocity gradient tensor.

Virtual experiment

As was first demonstrated by Moin and Spalart [13], a useful application of direct numerical simulation (DNS) of turbulence is to help improve the design of laboratory probes and to analyze their accuracy. This can be achieved by performing virtual experiments with a well resolved DNS database. The details about the database used in the present investigation are given in Vukoslavčević *et al.* [14], Vukoslavčević and Wallace [10], Vukoslavčević [11], Vukoslavčević and Wallace [3] and Vukoslavčević and Wallace [12], who analyzed the characteristics of single and multi-array hot-wire probes. Single array probes were also analyzed by Pompeo and Thomann [15] and Antonia *et al.* [16] using the same approach.

Although the parameters that affect the response of a hot-wire sensor, like finite sensor lengths, flow blockage by the presence of prongs and the thermal cross-talk between sensors, are not accounted for in this approach, it has provided real insight into the influence of the sensor and array configuration as well as the probe spatial resolution on the measurement accuracy.

To obtain the well resolved DNS, a minimal turbulent channel flow, similar to that of Jimenez and Moin [17], was simulated for a Reynolds number of $Re_\tau = 200$ where $Re_\tau = u_\tau h/v$, u_τ is the friction velocity and h is the channel half-width. The details of the numerical methodology can be found in Piomelli *et al.* [18]. The numerical grid was uniform in all directions, and the resulting resolution is $\Delta x^+ = \Delta y^+ = \Delta z^+ \approx 1$, where "+" denotes normalization with the viscous length v/u_τ. Near the wall the grid size is a little less than two-thirds of the Kolmogorov length in each coordinate direction and a little more than one-quarter of this length at the channel centerline.

Using this DNS database the sensors can be treated as points within the numerical mesh at the sensor centers. The positions of these points depend on the specific probe geometry, given in fig. 1, and the chosen probe spatial resolution to be simulated. This spatial resolution depends on the array center positions, defined by the distances of the array's center from the probe center, and on the distance from the array center to the sensor center.

The effective velocity, U_{eij}, cooling the *j*-th sensor of *i*-th array can be written in functional form as:

$$U_{eij}^2 = F(a_{ijk}, U_{ij}, V_{ij}, W_{ij}) \tag{1}$$

The specific form of this expression depends on various versions of the cooling laws. The a_{ijk} terms are calibration coefficients that can be determined from a calibration procedure for a real probe or theoretically for ideal sensor responses. The velocity components at each sensor center can be expressed as a function of the velocity components at the probe center, U_0, V_0, and W_0, and velocity gradients in the cross-stream y- and z-directions:

$$U_{eij}^2 = F_{ij}\{a_{ijk}, U_0, V_0, W_0, \partial(U,V,W)/\partial y, \partial(U,V,W)/\partial z\} \tag{2}$$

Using the velocity components at the virtual sensor centers from the DNS, U_{ij}, V_{ij}, and W_{ij}, the effective cooling velocity at each sensor center, U_{eij}, can be found from expression (1). The three velocity components at the probe center and the cross-stream velocity gradients can be obtained from the set of eqs. (2), by applying an adequate numerical algorithm

and assuming linear velocity variations over the probe sensing area. For sufficiently small probe dimension, the linear velocity variation is approximately true, so that the calculated values will be close to those of the DNS.

By comparing the statistical properties obtained from a virtual experiment in this way, for the various configurations of virtual probes, with the same properties determined directly from the DNS, the influence on the accuracy of velocity gradient measurements of the array and sensor geometrical arrangements, for a given spatial resolution, can be systematically examined. In addition, by varying the array separation and sensor size for a given probe geometry, the effects of spatial resolution also can be analyzed.

The accuracy of the cross-stream velocity gradient measurements

As stated in the previous section, the parameters that affect the accuracy of cross-stream velocity gradient measurements that we analyzed using virtual experiments are: the array arrangement within a probe sensing area, the sensor arrangements within an array, the probe spatial resolution and the ratio of the array to the array separation size. Each of these parameters is analyzed separately.

The influence of the array configuration

As discussed by Vukoslavčević and Wallace [3], in order to focus the analysis only on the effects of the array configurations and their spatial separations one can imagine perfect arrays that can exactly and simultaneously measure all three velocity components at their centers. Other sources of measurement errors, such as calibration errors (due to the complex form of sensor response, sensor dimensions, thermal cross-talk between sensors within an array, disturbance of the flow by the presence of the sensors and prongs), limited uniqueness range depending on number and orientations of the sensors, and electronic noise of instruments, were not considered. If the array separation is small enough to assume linear velocity variation between arrays, all the array configurations presented in fig. 1 with perfect arrays would give equal and accurate values of velocity and velocity gradient-based statistics at any referent point of the probe sensing area. Unfortunately, the experience of various probe designers has shown that fabricating multi-sensor probes small enough to achieve such linear velocity variation is practically impossible for even the most optimal laboratory conditions.

If the array separations are small enough to have either concave or convex variation of velocity component u_i between arrays, fig. 2(a), without the inflection point shown in fig. 2(b), the velocity derivative can be calculated using a finite difference:

$$u_i'(x) = \frac{u_i(x_2) - u_i(x_1)}{x_2 - x_1}$$

At a midpoint x the gradient is close to the exact value, but the velocity component that we can calculate there, is underestimated. It will be overestimated in the case of a concave variation between points x_1 and x_2.

The error in velocity determination at a given point can strongly affect the accuracy of velocity gradient determination at a given direction in a case of the multi-array probe configurations shown in fig. 1. For example, the velocity gradients in the z-direction, for the array configuration shown in fig. 1(a), would be in error because the velocity estimate at midpoint between array 1 and array 3 would be in error. The situation with the configuration shown in fig. 1(d) is similar, only the errors of velocity gradients in the z-direction will have opposite

Vukoslavčević, P. V., Wallace, J. M.: On the Accuracy of Measurement of Turbulent ...
THERMAL SCIENCE: Year 2017, Vol. 21, Suppl. 3, pp. S533-S551

S537

signs. By contrast with these configurations, the velocity gradients in the z-direction can be reasonably accurately estimated for the configuration shown in fig. 1(c), but the velocity gradient in y-direction could be in error for this configuration. In order to obtain the velocity gradients in the y- and z-directions with the same accuracy, the array configuration shown in fig. 1(f) can be used. However, due to the addition of an array, this configuration is more difficult to fabricate and operate. The gradients in both directions will be in error for the configuration shown in fig. 1(b). The configuration with five arrays, shown in fig. 1(e), has a referent point at its center with the simultaneous accuracy of the velocity components and velocity gradients in the y- and z-directions. Due to the presence of the central array the disadvantage of this configuration is much worse spatial resolution as well as much more complex fabrication and operation in comparison to the other configurations.

Figure 2. A nonlinear convex velocity variation (a), with an inflection point (b)
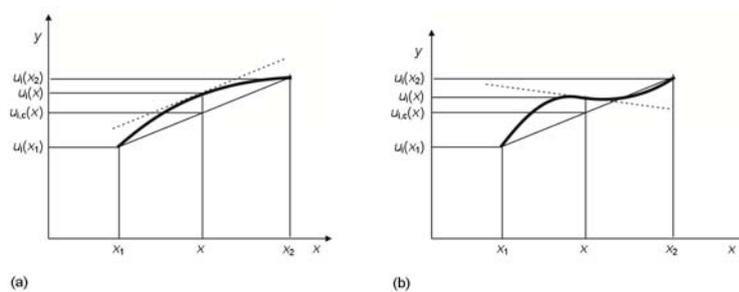
A virtual probe with the VW3-configuration and array distances, $a^+ = 8$ and $h^+ = 4$ is shown in fig. 3.

In order to "measure" the velocity gradients at the probe center in a virtual experiment it is necessary to know the velocity components at the array centers. In the case of probes with perfect arrays, they are equal to the velocity components from the DNS when the array centers coincide with the nodes of the grid. Otherwise an adequate interpolation procedure can be applied. If the array separation is small enough so that a linear velocity variation over probe sensing area can be assumed, the velocity gradient statistics measured this way will be the same as the one obtained from the DNS for all array arrangements. Otherwise, the difference will indicate the effects of the array geometrical arrangement on the measurement accuracy for a given spatial separation of the arrays.

In order to compare the various array configurations shown in fig. 1, the same spatial resolution (the distances between arrays) was maintained, i. e. $a^+ = 8$ and $h^+ = 4$, $\Delta^+ = 1$ for all configurations. The spatial resolution of probes with this array separation is close to or better than the best spatial resolution of any of the probes used in the experiments cited in chapter „*Introduction*". This means that the gradient measurement error in a physical experiment, due to array arrangements, will be close to or higher than the error obtained in a virtual experiment performed in this way. In fact, this is the minimal error because the influence of the sensor arrangement within the array and imperfection of the cooling law will
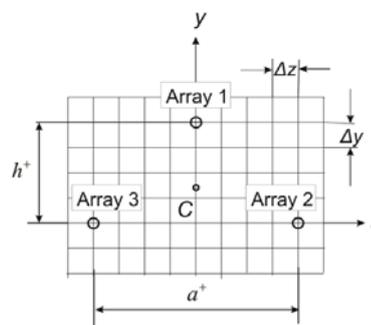

Figure 3. Sketch of a VW3-configuration with arrays shown as points on the DNS grid with $\Delta x^+ = \Delta y^+ = \Delta z^+ \approx 1$ resolution

increase the measurement error. It is possible that in some rare cases these errors are of opposite signs for some of the statistics, so they could cancel out, to some extent, but this will not generally be the case. If the technical difficulties are resolved and a probe of much smaller dimension can be fabricated, corresponding minimal error can be determined in a similar way.

For this channel flow DNS, $\eta/\Delta \approx 1.7$ at $y^+ = 15$ so that $a/\eta = 4.7$ and $h/\eta = 2.35$. These ratios increase closer to the wall and decrease toward the channel centerline. In the case of the TKD5 configuration, given in fig. 1, the distance from the probe to the array centers should be higher due to the presence of the central array. An average value of $a^+ = 10.4$ should be sufficient for most of the sensor configurations used so far.

The influence of the geometrical arrangements of the probe arrays, for a given spatial resolution, on the accuracy of the rms of the cross-stream velocity gradient measurements is presented in figs. 4 and 5 for the various array arrangements. Because the configuration TKD3 does not yield the best $\partial/\partial y$ or $\partial/\partial z$ gradient values, this configuration is not presented here.
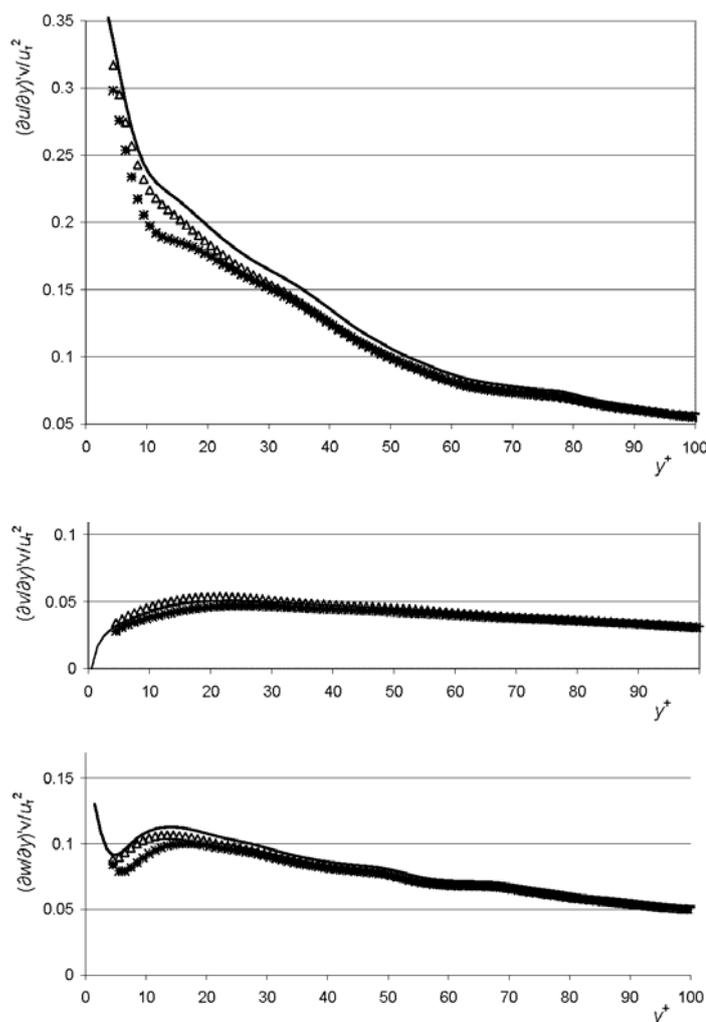

Figure 4. Effects of the array configurations, shown in fig. 1, on the velocity gradient component rms values in y-direction, all with $a^+ = 8$ and $h^+ = 4$;
*solid line DNS,
triangle VW3,
dash VWB3,
star HA3,
plus TKD4*

Vukoslavčević, P. V., Wallace, J. M.: On the Accuracy of Measurement of Turbulent ...
THERMAL SCIENCE: Year 2017, Vol. 21, Suppl. 3, pp. S533-S551

S539

As expected from fig. 2(a) and the discussion related to this figure, the accuracy of $\partial u_i/\partial y$ rms is the same for the configurations VWB3, HA3, and TKD4, as demonstrated in fig. 4. A similar result is seen in fig. 5 for $\partial u_i/\partial z$ for the VW3 and TKD4 configurations, although a slight difference is evident between the two cases due to the different position of the probe center with the respect to the array 2 and array 3 centers. The rms of $\partial u/\partial z$ of the VWB3 and HA3 configurations is overestimated. Due to the strong mean gradient of the U velocity component in the near the wall region, the U velocity component at midpoint of array 1 and array 3 of these configurations will be underestimated, as explained in fig. 2(a). As a consequence $\partial u/\partial z$ must be overestimated. The rms of $\partial w/\partial z$ is also overestimated with these configurations. This is due to the underestimated value of the rms of $\partial w/\partial y$ because of the insufficient probe spatial resolution in the y-direction. The effect is the same as in the case of the rms of $\partial u/\partial z$. So, the configurations VWB3 and HA3 are less accurate for most of the gradient rms measurements in comparison to the VW3 and TKD4 configurations. The accuracy of the $\partial u_i/\partial y$ rms is better in the case of VW3 than for the TKD4 configuration due to the better spatial resolution in the y-direction. Although none of the configurations presented here gives the best accuracy for the statistics of the all cross-stream velocity gradients, the VW3 configuration gives the best accuracy for $\partial u_i/\partial y$. It is slightly less accurate for the $\partial u_i/\partial z$
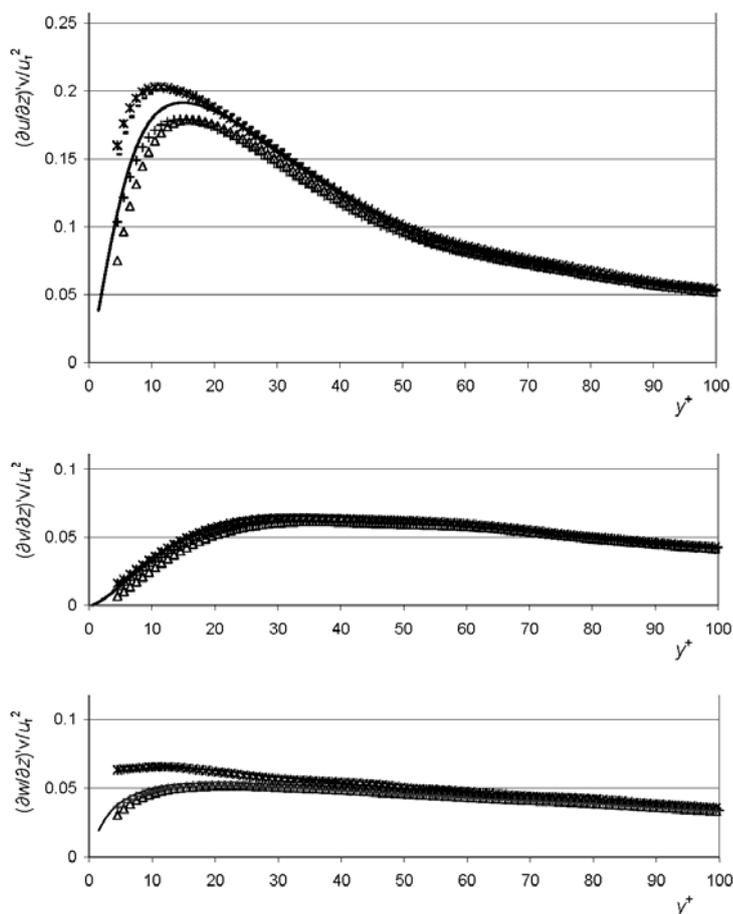

Figure 5. Effects of the array configurations, shown in fig. 1, on the velocity gradient component rms values in z-direction, all with $a^+ = 8$ and $h^+ = 4$;
solid line DNS, triangle VW3, dash VWB3, star HA3, plus TKD4

S540

Vukoslavčević, P. V., Wallace, J. M.: On the Accuracy of Measurement of Turbulent ...
THERMAL SCIENCE: Year 2017, Vol. 21, Suppl. 3, pp. S533-S551

gradients in comparison to TKD4 configuration, but much easier to construct and operate due to the smaller number of arrays and sensors.

Although the presented measurement accuracy is the best that can be achieved for the given spatial resolution, it is clear that the measurement error of some of the gradients is rather high. For example the minimal error of the $\partial u/\partial z$ rms is about 7% at $y^+ = 15$. In addition to this error, the error due to the finite array size and imperfection of the cooling law will be added in a real experiment.

The influence of the sensor configuration

Various sensor configurations within an array used so far as a part of multi-array or single array vorticity probes are presented in fig. 6.
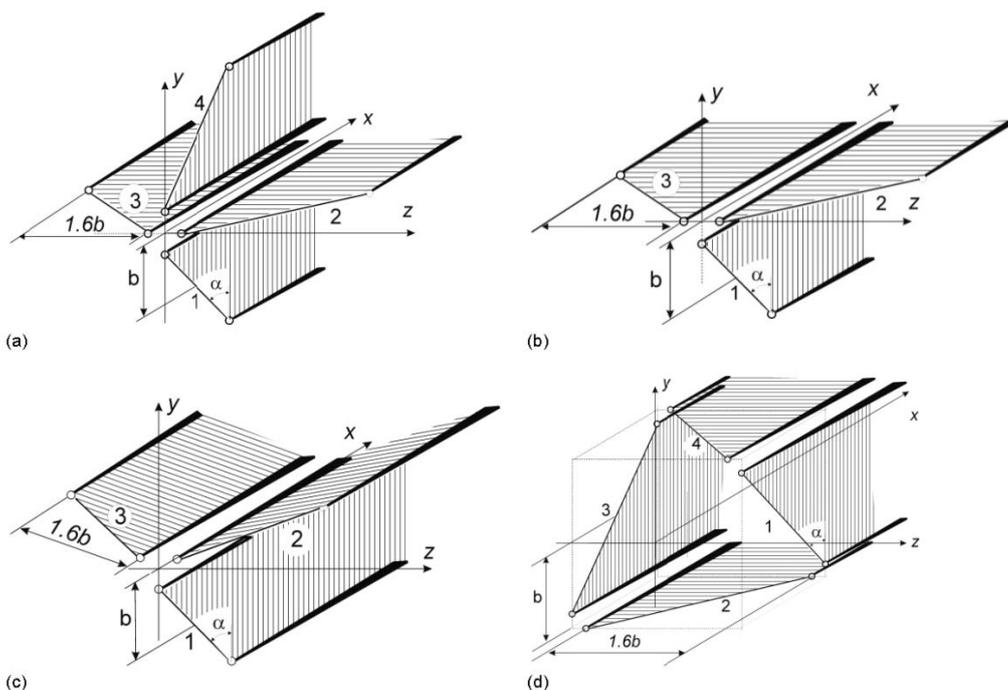

Figure 6. Various sensor configurations within an array to simultaneously measure all three velocity components; *(a) PL-plus configuration, (b) T-configuration, (c) OR-orthogonal configuration, (d) SQ-square configuration*

As a part of a multi-array vorticity probe, the *PL*-configuration was used by Tsinober *et al.* [5], Vukoslavčević and Wallace [6], Gulitski *et al.* [9] and Galanti *et al.* [8]. The *T*-configuration was used by Vukoslavčević *et al.* [4] in the first vorticity probes capable of simultaneous measurements of all three vorticity components. The *OR*-configuration was used by Honkan and Andreopoulos [7]. The *SQ*-configuration was used as a single array vorticity probe, capable of measuring the streamwise component of vorticity only, by Vukoslavčević and Wallace [19] and Kastrinakis and Eckelman [20]. The *SQ, PL* and *OR* configurations are also analyzed as a single array probes to measure all three velocity compo-

Vukoslavčević, P. V., Wallace, J. M.: On the Accuracy of Measurement of Turbulent ...
THERMAL SCIENCE: Year 2017, Vol. 21, Suppl. 3, pp. S533-S551

S541

nents by, among the others, Samet and Einav [21], Lekakis *et al.* [22], Holzapfel *et al.* [23], Dobbeling *et al.* [24] and Maciel and Gleyzes [25]. A single array consisting of an *X*-pair of sensors oriented in vertical planes and a *V*-pair in a horizontal plane was analyzed by Pompeo and Thoman [15]. The influence of the velocity variation on the measurement accuracy depends on the sensor arrangements. It has been studied in detail by Vukoslavčević [11]. He proposed a new, *XP*-configuration, consisting of an *X*-pair of sensors oriented in vertical planes and two parallel slanted sensors in horizontal planes. The measurements accuracy of this configuration should be less affected by the velocity gradients in comparison to the other configurations shown herein.

The testing of the influence of the sensor configurations on the accuracy of the velocity gradient measurement can be performed for various array configurations and various array separations, which would lead to a large number of virtual experiments. A reasonable choice to start with would be the most promising array configuration discussed in previous chapter, *i. e.* VW3. The spatial resolution with this probe design of $h^+ = 10$ and $a^+ = 11.5$ was achieved in the boundary layer experiment of Vukoslavčević and Wallace [6]. It is possible to further improve the spatial resolution by reducing the prongs and array separation almost in half. However, to go below $h^+ = 6$ and $a^+ = 6.8$, corresponding to a critical sensor length to diameter ratio close to 200, with minimal prong separations at array centers does not seem realistic. Based on our experience in constructing this type of probe, thermal and aerodynamical cross-talk between sensors and prongs can be expected even with this separation. It would be possible to further improve the spatial resolution using 1 micron sensor diameters in place of the 2.5 micron that have been used so far. We believe that technical difficulties in constructing such a probe can be resolved, but the thermal and aerodynamical cross-talk between sensors and prongs can be serious problems in this case. With these considerations in mind, we chose a spatial resolution of $h^+ = 6$ and $a^+ = 6.8$, as was also done by Vukoslavčević and Wallace [12]. A sketch of a VW3 probe with this resolution and the PL sensor configuration, placed over the numerical grid is shown in fig. 7.

Testing the influence of various sensor configurations is performed by replacing the *PL* with *SQ*, *OR*, and *XP* configurations. The T configuration is a part of *PL* configuration, so it is not tested separately. The results are presented in fig. 8 and fig. 9.

The sensor configurations used so far for vorticity probes designs were *PL* and *OR*. It is clear that the $\partial v/\partial y$ and $\partial w/\partial z$ gradients are strongly in error with these configurations. Fortunately these two gradients do not affect the accuracy of any of the vorticity components. This was a fortunate coincidence that the designers of the vorticity probes probably were not aware of when they made the choice of the sensor configurations. The rms of the $\partial u/\partial y$ and $\partial u/\partial z$ gradients are almost unaffected by the
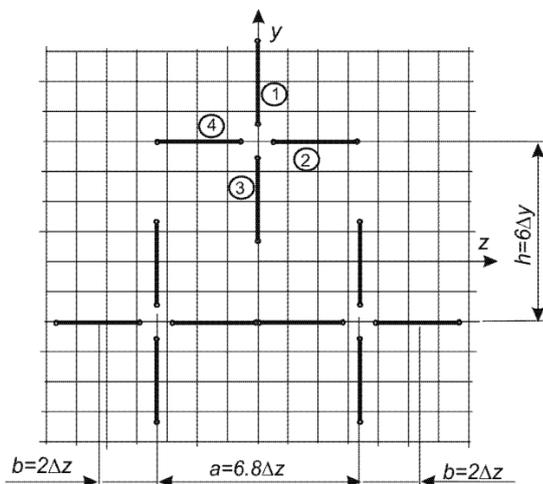

Figure 7. Virtual presentation of the VW3 12-sensor probe with the PL sensor configuration

S542

Vukoslavčević, P. V., Wallace, J. M.: On the Accuracy of Measurement of Turbulent ...
THERMAL SCIENCE: Year 2017, Vol. 21, Suppl. 3, pp. S533-S551

sensor arrangements. It is interesting that in the case of $\partial w/\partial y$ the errors due to the array configuration and sensor configuration are of opposite signs. They practically cancel out for the *PL* configuration. The rms of the $\partial v/\partial z$ gradient is much more accurate for the *PL* compared to the *OR* or *SQ* configurations. It turns out that the *PL* configuration, which was the choice most used in the design of vorticity probes, was the best choice among the available configurations at that time. The rms values obtained with the new proposed *XP* configuration are practically the same as the ones obtained by a virtual perfect array. The sensor configuration
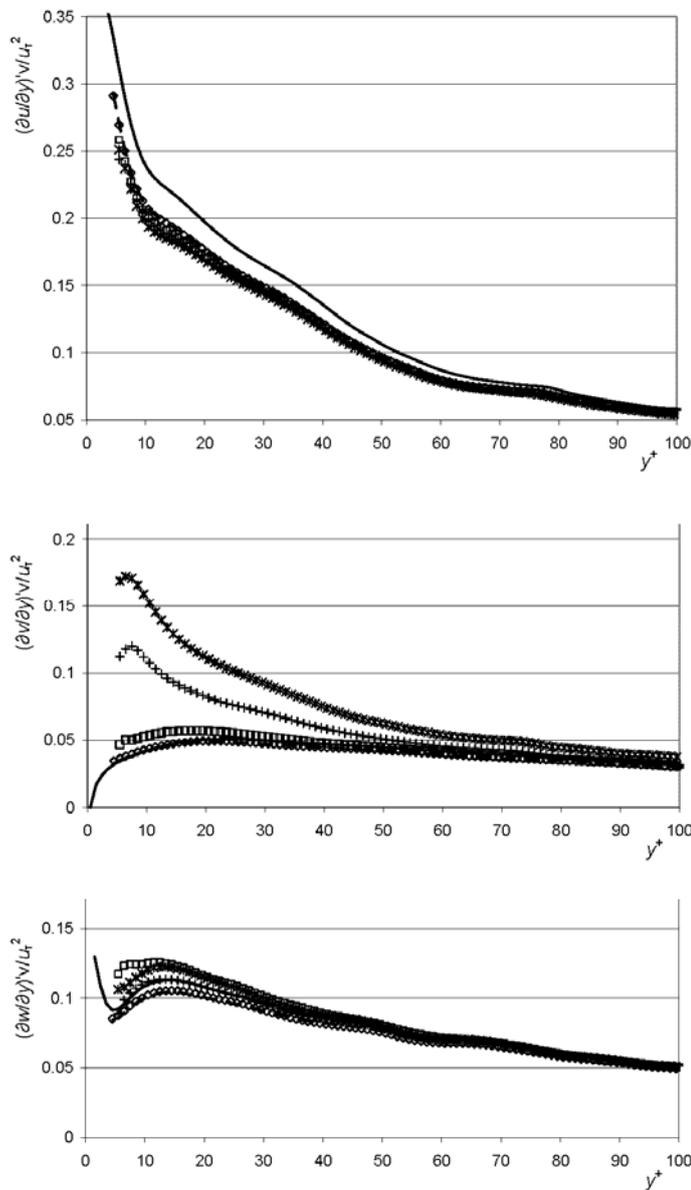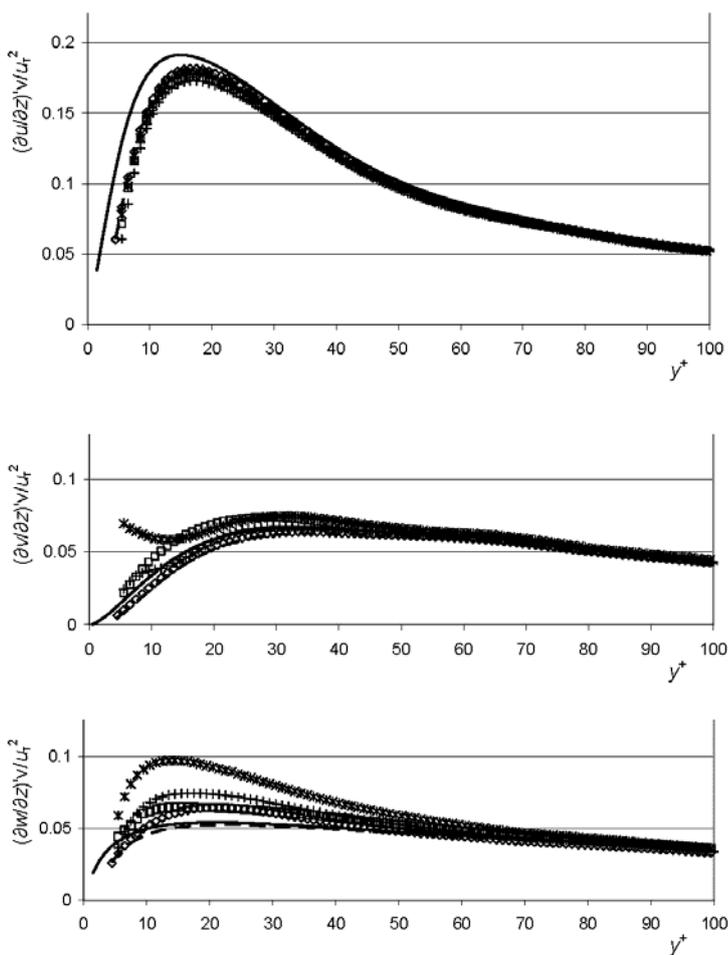

Figure 8. Effects of the sensor configurations, shown in fig. 6, on the velocity gradient component rms values in the y-direction, all with $h^+ = 6$ and $a^+ = 6.8$;
solid line DNS,
plus PL,
star OR,
square SQ,
diamond XP,
dash perfect array

Vukoslavčević, P. V., Wallace, J. M.: On the Accuracy of Measurement of Turbulent ...
THERMAL SCIENCE: Year 2017, Vol. 21, Suppl. 3, pp. S533-S551

S543

does not add any error in this case. Although this configuration looks to be the most promising, the influences of thermal and aerodynamic cross-talk as well as the uniqueness range for this configuration are not clarified yet.

Figure 9. Effects of the sensor configurations, shown in fig. 6, on the velocity gradient component rms values in the z-direction, all with $h^+ = 6$ and $a^+ = 6.8$;
solid line DNS,
plus PL,
star OR,
square SQ,
diamond XP,
dash perfect array

The influence of the probe spatial resolution

The effects of the spatial resolution of the probe depend on the array as well as on the sensor configurations. Examining all possible combinations requires a very large number of virtual experiments. Rather than attempting that, we have chosen the array and sensor configurations that appear to be most promising and then have proportionally varied their size. As previously discussed, the *VW3* array configuration looks to be the most promising one. The most frequently used sensor configuration for vorticity probes was the *PL* configuration. As shown in previous chapter, it is more accurate than the *OR* configuration, which was also used in a vorticity probe design. Although the *XP* sensor configuration shows great promise, it has not been used so far. Therefore, the *PL* configuration is the choice we will examine in this analysis.

S544

Vukoslavčević, P. V., Wallace, J. M.: On the Accuracy of Measurement of Turbulent ...
THERMAL SCIENCE: Year 2017, Vol. 21, Suppl. 3, pp. S533-S551

As shown in fig. 7, the characteristic probe dimensions are the array separations, a and h and the sensor centers separation b. We decided to start from $a^+ = h^+ = 9$ and $b^+ = 2$, separations that are slightly better than the best spatial resolution of this type of the probe used so far for boundary layer measurements. We then proportionally increase the probe's spatial resolution. As discussed in previous chapter, by reducing the array separation and choosing a sensor diameter of 1 micron in place of the 2.5 micron wire, theoretically it is possible to construct a probe with dimensions close to $a^+ = h^+ = 3$. Although constructing a probe of this size does not seem realistic at this time, it is worthwhile studying its spatial resolution as a guideline for future designs. The results of the effects of the probe spatial resolution on the cross-stream velocity gradients are presented in fig. 10 and fig. 11. All other array and sensor configurations as well as the probe spatial resolution can be studied in a similar way.
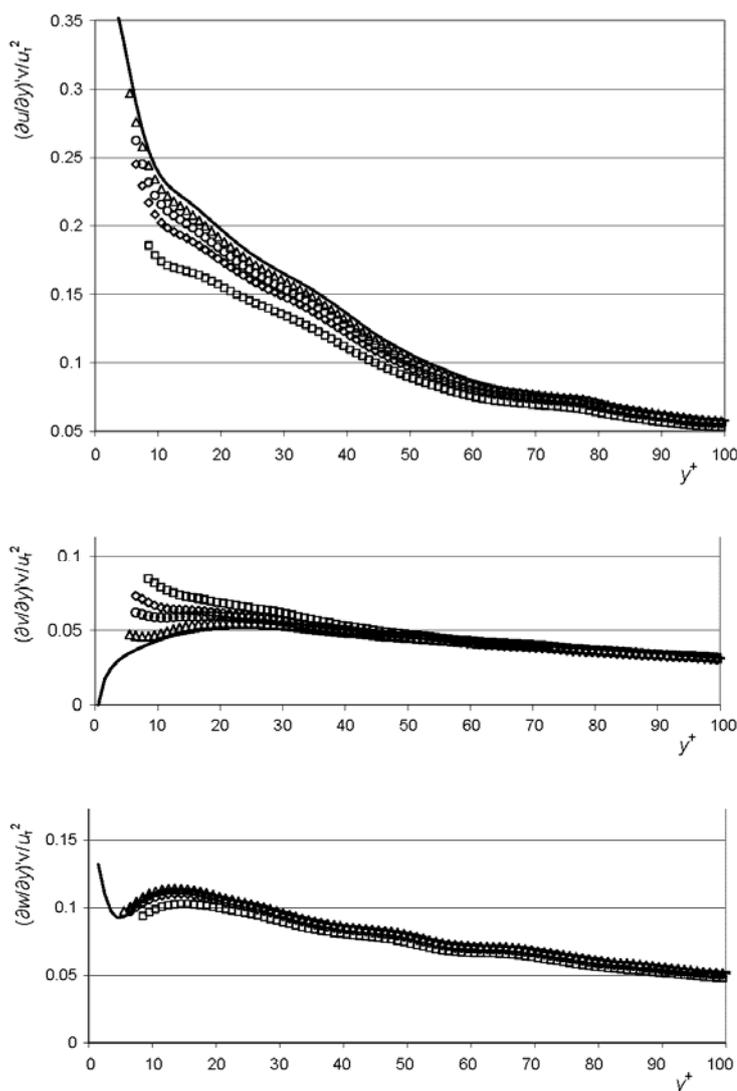

Figure 10. Effects of the probe spatial resolution, on the velocity gradient component rms values in the y-direction for the VW3 array and the PL sensor configuration; *solid line DNS, square $a^+ = h^+ = 9$, diamond $a^+ = h^+ = 6$, circle $a^+ = h^+ = 4.5$, triangle $a^+ = h^+ = 3$*

Vukoslavčević, P. V., Wallace, J. M.: On the Accuracy of Measurement of Turbulent ...
THERMAL SCIENCE: Year 2017, Vol. 21, Suppl. 3, pp. S533-S551

S545

A strong influence of the probe spatial resolution for $a^+ = h^+ > 4.5$ for the most of the velocity gradient components is evident. The most affected are the $\partial u/\partial y$ and $\partial v/\partial y$ gradients, which is typical for the *PL* sensor configuration. The $\partial u/\partial y$ gradient is about 8% in error at $y^+ = 15$ and $\partial v/\partial y$ about 17%. Fortunately, the $\partial v/\partial y$ does not affect the vorticity measurement accuracy. For the best spatial resolution, $a^+ = h^+ = 3$, the virtual probe approximates the DNS gradient values very well.

Figure 11. Effects of the probe spatial resolution, on the velocity gradient component rms values in the z-direction for the VW3 array and the PL sensor configuration;
solid line DNS,
square $a^+ = h^+ = 9$,
diamond $a^+ = h^+ = 6$,
circle $a^+ = h^+ = 4.5$,
triangle $a^+ = h^+ = 3$
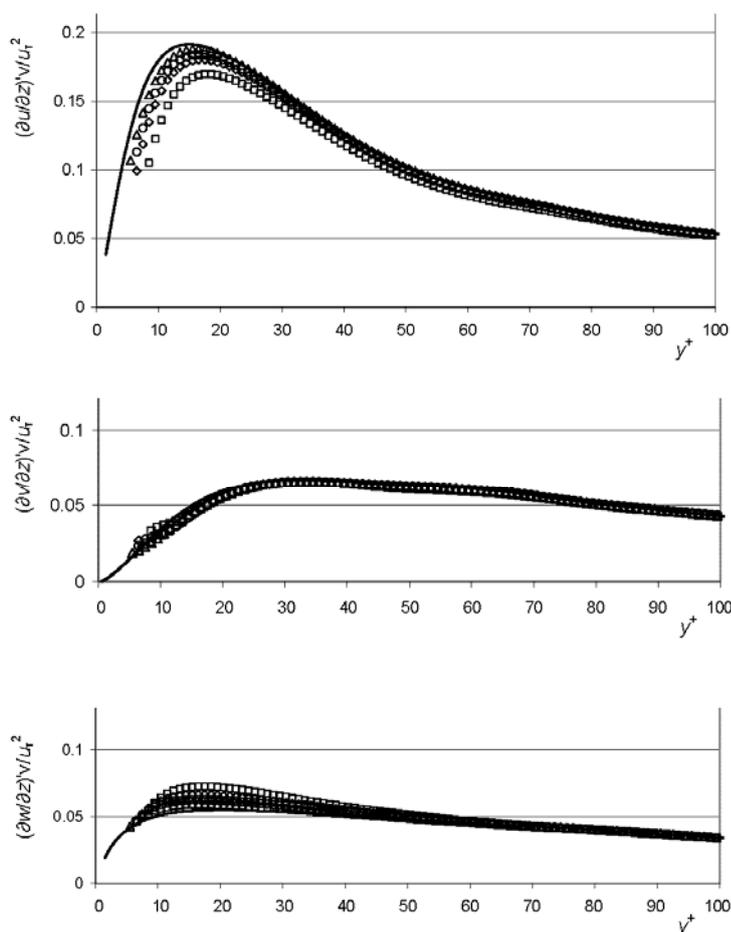
The influence of the ratio of the array to the array separation size

As discussed in previous section, in order to study the probe spatial resolution, the array size and array separation are reduced proportionally. By reducing the array size the error in velocity measurements, due to the sensor configuration and separation, will be reduced which will increase the accuracy of velocity gradient measurements. On the other hand, reducing the array separation results in the error in velocity measurements increasing the error in the velocity gradient measurements. So, it is not clear in advance whether the error in velocity gradient measurements will decrease or increase by proportional decreasing the probe

S546

Vukoslavčević, P. V., Wallace, J. M.: On the Accuracy of Measurement of Turbulent ...
THERMAL SCIENCE: Year 2017, Vol. 21, Suppl. 3, pp. S533-S551

dimensions. In order to study this effect the $\partial v/\partial y$ gradient is analyzed. The measurement error of this gradient is higher than the measurement errors of the other gradients, for the same probe dimensions, as shown in fig. 10. The influences of four different ratios of array to array separation size are presented in fig. 12.
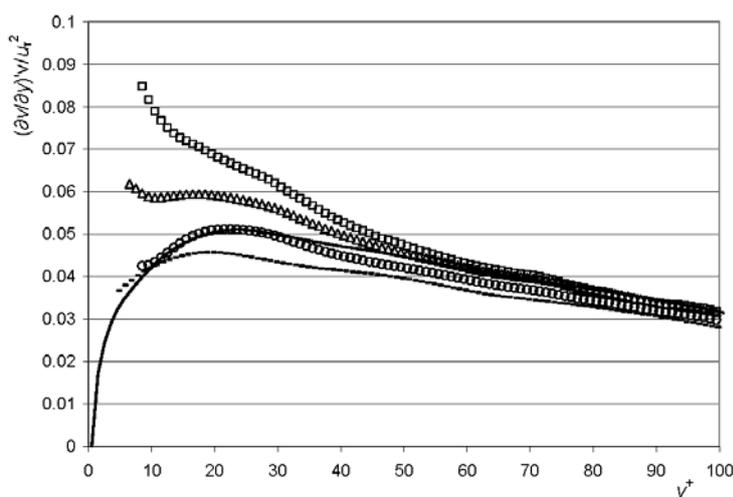

Figure 12. Effects of the various ratios of array to array separation size for the VW3 array and the PL sensor configuration;
solid line DNS, square $a^+ = h^+ = 9$ and $b^+ = 2$, triangle $a^+ = h^+ = 4.5$ and $b^+ = 1$, circle $a^+ = h^+ = 9$ and $b^+ = 1$, dash $a^+ = h^+ = 9$ and $b^+ = 0$ (perfect array)

In a case of $a^+ = h^+ = 9$ and $b^+ = 2$, the measurement error is about 25% at $y^+ = 20$. By reducing all dimensions in half ($a^+ = h^+ = 4.5$ and $b^+ = 1$), the error is decreased to 16%. Keeping the array separation unchanged and reducing the array size in half ($a^+ = h^+ = 9$ and $b^+ = 1$), the measurement error is practically zero. Reducing the array size to zero and thus eliminating the error due to the finite array size, the measurement error is about -11%. This is the error due to the array separation only. It is clear that the errors due to the array separation and array size are of the opposite signs. In this case they cancel out if the array separation is $a^+ = h^+ = 9$ and array size $b^+ = 1$. So in the case of $\partial v/\partial y$ it is better to reduce the sensor separation only rather than reducing all probe dimensions proportionally. An optimal ratio of these separations obviously exists. The other gradients are affected differently. A general approach to optimize the measurement accuracy of all gradients simultaneously does not appear to exist. Optimization depends on the array configuration and the technical possibilities to construct a probe of a given dimensions.

The accuracy of the streamwise velocity gradient measurements

The only probe capable of direct streamwise velocity gradient measurements is the *TKD5* configuration shown in fig. 1. It has the central array moved upstream of the other four arrays for some distance Δx. A detailed investigation of the influence of the array configuration of this probe on the accuracy of the streamwise velocity gradient measurements was done by Vukoslavčević and Wallace [3]. They showed that all three gradients $\partial u_i/\partial x_i$ are greatly in error, even for the best spatial resolution that can be practically achieved. These errors are

Vukoslavčević, P. V., Wallace, J. M.: On the Accuracy of Measurement of Turbulent ...
THERMAL SCIENCE: Year 2017, Vol. 21, Suppl. 3, pp. S533-S551

S547

over 100% at $y^+ = 15$. An additional error due to the finite array size and various factors that can affect probe calibration, will add to this error. It may happen that some of these errors have opposite signs, but to expect to cancel out an error of over 100% is not likely. They also analyzed a possibility of indirect measuring of the $\partial u/\partial x$ gradient using the continuity equation by:

$$\left(\frac{\partial U}{\partial x}\right)_c = -\frac{\partial V}{\partial y} - \frac{\partial W}{\partial z} \tag{3}$$

for various array configurations.

Assuming that the gradients $\partial V/\partial y$ and $\partial W/\partial z$ are measured with sufficient accuracy, the $\partial U/\partial x$ gradient can be calculated from eq. (3) and used to test Taylor's hypothesis:

$$\left(\frac{\partial U}{\partial x}\right)_T = -\frac{1}{U_{con}}\frac{\partial U}{\partial t} \tag{4}$$

for a given value of convective velocity, U_{con}. This expression can be also used to determine the appropriate value of U_{con}, assuming that the $(\partial U/\partial x)_c$ is determined with sufficient accuracy. In order to test these possibilities, Vukoslavčević and Wallace [3] analyzed the influence of various array configuration on the accuracy of rms of $(\partial U/\partial x)_c$. They found that the influence of the array configuration is almost negligible for the *VW3* configuration. All other configurations are strongly in error, especially the *VWB3* and *HA3* configurations. In order to get real insight into the possibility of using this configuration to measure $(\partial U/\partial x)_c$, it is necessary to simultaneously examine the influence of the array size and sensor configuration on the measurement accuracy.

The rms of $(\partial U/\partial x)_c$ is compared in fig. 13 for the *PL* and *SQ* sensor configurations and the *VW3* array configuration.

Although the influence of the array configuration is negligible, the influence of the sensor configuration is very large for both the *PL* and *SQ* configurations. The error is over 100% at a distance of $y^+ = 15$ from the wall.

From this it is clear that neither direct nor indirect measurement of any of streamwise velocity gradients is possible with multi-sensor hot-wire probe with sufficient accuracy.
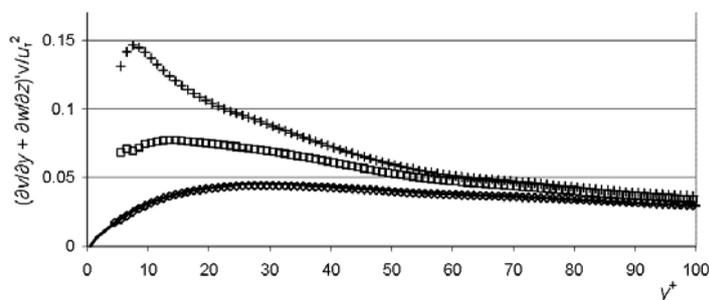

Figure 13. Effects of the sensor configurations, shown in fig. 6, on the $(\partial U/\partial x)_c$ velocity gradient rms values for the VW3 array configuration, all with $h^+ = 6$ and $a^+ = 6.8$;
solid line DNS, diamond zero array size, plus PL, square SQ

Fortunately, these gradients can be accurately determined using Taylor's hypothesis by choosing an appropriate value of convective velocity except near the wall [26].

Comparison of the virtual and physical experiments

In order to compare a virtual and physical experiment it is necessary to perform both of them under the same conditions. Building a set of vorticity probes with various array and sensor configurations, sizes and separations and then performing a physical experiment, like the virtual one presented in two previous chapters, is a very complex task that has not been attempted to date. The only experiment of this type was performed by Antonia *et al*. [16] with a probe capable of measuring the $\partial U/\partial y$ velocity gradient only. The probe consisted of two parallel sensors separated by a distance Δy. The statistical variances of $\partial U/\partial y$ fluctuations, for a channel flow, were compared for various sensor separations in a physical and virtual experiment. The results obtained at the channel centerline are shown in fig. 14.

The comparison of the virtual and physical results is excellent for $\Delta y^* > 2$, where $\Delta y^* = \Delta y/\eta$ is the sensor separation scaled by Kolmogorov microscale. This means that, in this range, the virtual experiments can be successfully used to analyze the performance of this type of probe. A difference from unity in this region is a measure of the attenuation of the physically measured rms values of the gradient due to insufficient probe spatial resolution. For example, with a sensor separation of about four Kolmogorov scales the error is about 10%. For $\Delta y^* < 2$ an increasing difference between the virtual and physical data is evident. This difference goes to infinity when $\Delta y^* \to 0$. In a physical experiment some error in the velocity measurement will always occur. Even in a case of perfect calibration, when the influence of thermal crosstalk and aerodynamic blockage are fully taken into account, a small error due to electrical noise will be present. When this small error in velocity measurement is divided by the inexactly known small sensor separation, a large velocity gradient error results, going toward infinity for a sensor separation close to zero. A probe with two parallel sensors, like the one used in this experiment, can measure the U velocity component only by neglecting the influence of the V and W components. If the influence of these components is significant, a difference between physical and virtual experiments must appear, but this difference is small for the data shown in fig. 14. The W component is aligned with both sensors, so its influence is negligible. At the channel centerline, both sensors should be equally affected by the V velocity component. Therefore, the $\partial U/\partial y$ gradient, measured in the physical experiment referred to in fig. 14 should not be affected by neglecting these two velocity components for measurements at the
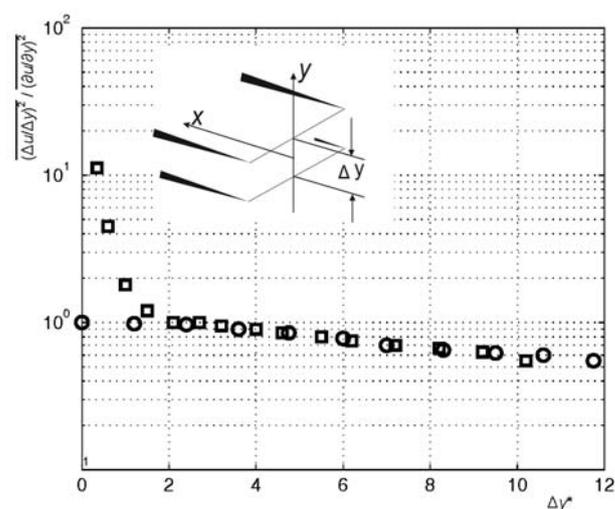

Figure 14. Comparison of physical (□) velocity gradient fluctuation variances to DNS simulated values (○) at the channel centerline for varying separations over which the velocity difference was determined [16]

Vukoslavčević, P. V., Wallace, J. M.: On the Accuracy of Measurement of Turbulent ...
THERMAL SCIENCE: Year 2017, Vol. 21, Suppl. 3, pp. S533-S551

S549

channel centerline. So the physical and virtual data should match well, as is the case for $\Delta y^* > 2$.

To perform an experiment similar to the one of Antonia *et al.* [16] with a vorticity probe would be an enormous task. Even if a set of these probes with various array separation distances were constructed, it does not seem realistic to reduce the array separations below $h^* = 6$ at $y^+ = 15$. The array separation in a case of vorticity probes is equivalent to the sensor separation Δy^* of Antonia *et al.* [16]. So, the only possibility to compare a physical and virtual experiment at the present time is to use some experimental results obtained by vorticity probes of a given spatial resolution, similar to the results from the virtual experiment shown in two previous chapters. Most vorticity probe data has been obtained in turbulent boundary layer experiments. However, the statistics of these channel and boundary layer flows are similar in the wall region, so a comparison of the distribution of the rms values of the $\partial U/\partial y$ variance in this region should provide an indication of the usefulness of the virtual experiment.

In fig. 15, the virtual channel flow data of $\partial u/\partial y$ rms, for various array separations are compared to the boundary layer data of Balint *et al.* [27] obtained with the *VBW3* vorticity probe. The array separation in the y-direction of this probe was $h^+ = 10.9$. The results compare very well with the virtual one obtained by a probe with array separation of $h^+ = 9$. Keeping in mind the uncertainty in the determination of u_t, as discussed by Ong and Wallace [28], the difference in flow characteristics and array separations, the agreement between the virtual and physical experiments is surprisingly good. The comparisons in figs. 14 and 15 indicate that virtual probe experiments can serve as a good tool to assist in the design and analysis of complex probes, an idea first put forward by Moin and Spalart [13].

Figure 15. Comparison of the channel flow virtual and boundary layer flow physical experiments of $\partial u/\partial y$ rms for the VW3 array configuration;
solid line DNS,
square $a^+ = h^+ = 9$,
diamond $a^+ = h^+ = 6$,
circle $a^+ = h^+ = 4.5$,
triangle $a^+ = h^+ = 3$ and
boundary layer experiment of Balint at al. [27],
($a^+ = h^+ = 10.9$) full diamond
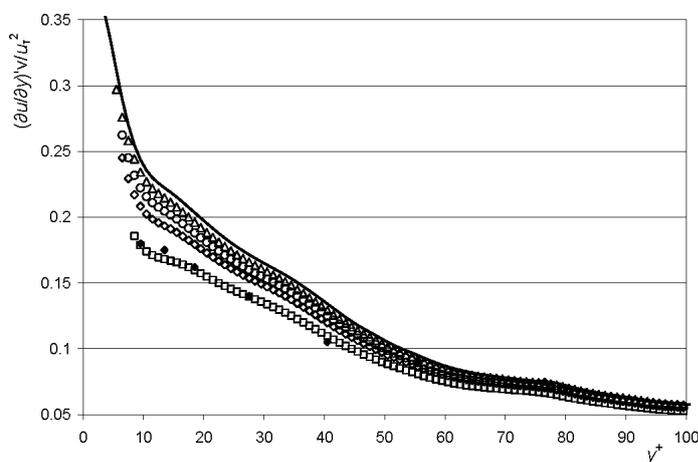
Conclusions

- Virtual experiments using a well resolved DNS database can serve as a good tool to examine the capability of various multi-sensor probe designs to measure the components of the velocity gradient tensor.
- The probe spatial resolution as well as the array and sensor configurations strongly affect the accuracy of the measured velocity gradient statistics. No unique configuration exists that gives the best accuracy for all components of velocity gradients.

- It appears that the plus sensor configuration, the one most frequently used thus far to measure vorticity components, was the best choice for that purpose.
- Most vorticity probes used thus far can measure the $\partial u/\partial y$, $\partial u/\partial z$, $\partial v/\partial z$, $\partial w/\partial y$ velocity gradients needed to determine all the vorticity components with reasonable accuracy. None of these probes can measure $\partial v/\partial y$ and $\partial w/\partial z$ gradients with sufficient accuracy.
- The only probe designed to directly measure the streamwise velocity gradients cannot measure them with sufficient accuracy, even with the best spatial resolution that is possible to achieve at the present time. It looks as if simultaneous measurements of streamwise and cross-stream velocity gradients is impossible with sufficient accuracy using multi-array hot-wire probes.
- The ratio of the array and array separation sizes strongly affects the accuracy of some of the gradient measurements. An optimal ratio is evident for some of the gradients.

Acknowledgment

References

[1] Taylor, G. I., Production and Dissipation of Vorticity in a Turbulent Fluid, *Proc. R. Soc. London, Ser. A, 164* (1938), 916, pp. 15-23
[2] Wallace, J. M., Vukoslavčević, P. V., Measurement of the Velocity Gradient Tensor in Turbulent Flows, *Annu. Rev. Fluid Mech., 42* (2010), Jan., pp. 157-181
[3] Vukoslavčević, P. V, Wallace, J. M., The Influence of the Arrangements of Multi-Sensor Probe Arrays on the Accuracy of Simultaneously Measured Velocity and Velocity Gradient-Based Statistics in Turbulent Shear Flows, *Exp. Fluids, 54* (2013), 6, ID 1537
[4] Vukoslavčević, P., et al., The Velocity and Vorticity Vector Fields of a Turbulent Boundary Layer. Part 1. Simultaneous Measurement by Hot Wire Anemometry, *J. Fluid Mech., 228* (1991), July, pp. 25-51
[5] Tsinober, A., et al., Experimental Investigation of the Field of Velocity Gradients in Turbulent Flows, *J. Fluid Mech., 242* (1992), Sept., pp. 169-192
[6] Vukoslavčević, P., Wallace, J. M., A 12-sensor Hot-Wire Probe to Measure the Velocity and Vorticity Vectors in Turbulent Flow, *Meas. Sci. Technol., 7* (1996), 10, pp. 1451-1461
[7] Honkan, A., Andreopoulos, Y., Vorticity, Strain Rate and Dissipation Characteristics in the Near Wall Region of Turbulent Boundary Layers, *J. Fluid Mech., 350* (1997), Nov., pp. 29-96
[8] Galanti, B., et al., Velocity Derivatives in Turbulent Flows in an Atmospheric Boundary Layer without Taylor Hypothesis, *Proceedings* (Eds. N. Kasagi *et al.*), Third International Symposium on Turbulence and Shear Flow Phenomena (TSFP3), Sendai, Japan, 2003, Vol. II, pp. 745-750
[9] Gulitski, G., et al., Velocity and Temperature Derivatives in High-Reynolds Number Turbulent Flows in the Atmospheric Surface Layer. Part 1. Facilities, Methods and Some General Results, *J. Fluid Mech., 589* (2007), Oct., pp. 57-81
[10] Vukoslavčević, P. V., Wallace, J. M., On the Accuracy of Simultaneously Measuring Velocity Component Statistics in Turbulent Wall Flows with Arrays of Three or Four Hot-Wire Sensors, *Exp. Fluids, 51* (2011), 6, pp. 1509-1519
[11] Vukoslavčević, P. V., A Hot-Wire Probe Configuration and Data Reduction Method to Minimize Velocity Gradient Errors for Simultaneous Measurement of Three Velocity Components in Turbulent Flows, *Exp. Fluids, 53* (2012), 2, pp. 481-488
[12] Vukoslavčević, P. V., Wallace, J. M., Using Direct Numerical Simulation to Analyze and Improve Hot-Wire Probe Sensor and Array Configurations for Simultaneous Measurement of the Velocity Vector and the Velocity Gradient Tensor, *Phys. Fluids, 25* (2013), 11, ID 110820

Vukoslavčević, P. V., Wallace, J. M.: On the Accuracy of Measurement of Turbulent ...
THERMAL SCIENCE: Year 2017, Vol. 21, Suppl. 3, pp. S533-S551

S551

[13] Moin, P., Spalart, P. R., Contributions of Numerical Simulation Data Bases to the Physics, Modeling and Measurement of Turbulence, NASA-TM-100022, NASA Ames Research Center, Moffett Field, Cal., USA, 1987

[14] Vukoslavčević, P. V., *et al*., On the Spatial Resolution of Velocity and Velocity Gradient-Based Turbulence Statistics Measured with Multi-Sensor Hot-Wire Probes, *Exp. Fluids*, *46* (2009), 1, pp. 109-119

[15] Pompeo, L., Thomann, H., Quadruple Hot-Wire Probes in a Simulated Wall Flow, *Exp. Fluids*, *14* (1993), 3, pp. 145-152

[16] Antonia, R. A., *et al*., On the Measurement of Lateral Velocity Derivatives in Turbulent Flows, *Exp. Fluids*, *15* (1993), 1, pp. 65-69

[17] Jimenez, J., Moin, P., The Minimal Flow Unit in Near-Wall Turbulence, *J. Fluid Mech.*, *225* (1991), Apr., pp. 213-240

[18] Piomelli, U., *et al*., Turbulent Structures in Accelerating Boundary Layers, *Journal of Turbulence*, *1* (2000), 1, pp. 1-16

[19] Vukoslavčević, P., Wallace, J. M., Influence of Velocity Gradients on Measurements of Velocity and Streamwise Vorticity with Hot-Wire X-Array Probes, *Rev. Sci. Instrum.*, *52* (1981), 6, pp. 869-879

[20] Kastrinakis, E. G., Eckelmann, H., Measurements of Streamwise Vorticity Fluctuations in a Turbulent Channel Flow, *J. Fluid Mech.*, *137* (1983), Dec., pp. 165-186

[21] Samet, M., Einav, S., A Hot-Wire Technique for Simultaneous Measurement of Instantaneous Velocities in 3D Flows, *J. Phys. E: Sci. Instrum.*, *20* (1987), 6, pp. 683-690

[22] Lekakis, I. C., *et al*., Measurement of Velocity Vectors with Orthogonal and Non-Orthogonal Triple-Sensor Probes, *Exp. Fluids*, *7* (1989), 4, pp. 228-240

[23] Holzapfel, F., *et al*., Assessment of a Quintuple Hot-Wire Technique for Highly Turbulent Flows, *Exp. Fluids*, *18* (1994), 1, pp. 100-106

[24] Dobbeling, K., *et al*., Basic Considerations Concerning the Construction and Usage of Multiple Hot-Wire Probes for Highly Turbulent Three-Dimensional Flows, *Meas. Sci. Technol.*, *1* (1990), 9, pp. 924-933

[25] Maciel, Y., Gleyzes, C., Survey of Multi-Wire Probe Data Processing Techniques and Efficient Processing of Four Wire Probe Velocity Measurements in Turbulent Flows, *Exp. Fluids*, *29* (2000), 1, pp. 66-78

[26] Geng, C., *et al*., Taylor's Hypothesis in Turbulent Channel Flow Considered Using a Transport Equation Analysis, *Phys. Fluids*, *27* (2015), 2, ID 025111

[27] Balint, J. L., *et al*., The Velocity and Vorticity Vector Fields of a Turbulent Boundary Layer. Part 2: Statistical Properties, *J. Fluid Mech.*, *228* (1991), July, pp. 53-86

[28] Ong, L., Wallace, J. M., Joint Probability Density Analysis of the Structure and Dynamics of the Vorticity Field of a Turbulent Boundary Layer, *J. Fluid Mech.*, *367* (1997), July, pp. 291-328